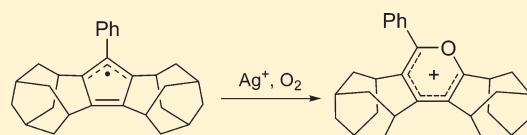


Allyl Radical Nature of a Phenylcyclopentadienyl Radical Annulated with Two Homoadamantene Frameworks

Kohei Ogawa,[†] Koichi Komatsu,^{†,‡} and Toshikazu Kitagawa^{*,§}[†]Institute for Chemical Research, Kyoto University, Uji, Kyoto 611-0011, Japan[‡]Department of Environmental and Biological Chemistry, Fukui University of Technology, Gakuen, Fukui 910-8505, Japan[§]Department of Chemistry for Materials, Graduate School of Engineering, Mie University, Tsu, Mie 514-8507, Japan

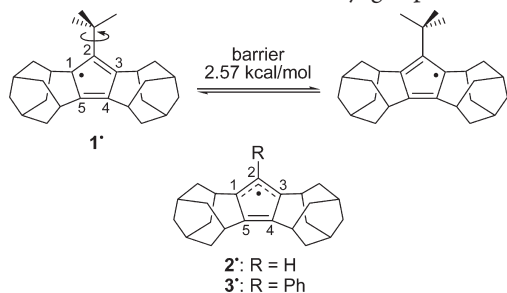
S Supporting Information

ABSTRACT: 1-Phenylcyclopentadiene fused with two homoadamantene units at the 2,3- and 4,5-positions (**4**) was deprotonated with KH to lead to the quantitative formation of the corresponding cyclopentadienyl (Cp) anion **3[−]**. This anion was oxidized by AgCl to afford an orange crystalline solid consisting of Cp radical **3[•]** and cyclopentadiene **4**. The ESR spectrum in hexane exhibited approximately 15 lines, demonstrating that the two homoadamantene frameworks were equivalent and that the C1–C2(Ph)–C3 moiety of the five-membered ring formed a symmetrical allyl-like radical in agreement with the prediction by DFT calculation. The reaction of the Cp radical **3[•]** with an oxygen molecule in the presence of Ag⁺SbF₆[−] afforded the SbF₆[−] salt of a phenylpyrylium ion annulated with two homoadamantene frameworks (**8⁺**SbF₆[−]).



INTRODUCTION

The cyclopentadienyl (Cp) radical is an important intermediate and building block in organic and organometallic chemistry.¹ Thus, the investigation of its electronic structure is a topic of fundamental significance. A variety of theoretical studies have shown that the doubly degenerated ground state of a pentasubstituted Cp radical C₅R₅[•] with a D_{5h} geometry will be subjected to Jahn–Teller distortion and will result in a less symmetric C_{2v} configuration.^{2,3} Such a distorted radical was observed by ESR spectroscopy only at low temperature in matrices because the conformational changes occur through an extremely low energy barrier.^{3–5} On the other hand, in monosubstituted Cp radicals,⁶ an electronic perturbation of the substituent brings about a loss of the degeneracy to result in a non-equivalent spin distribution on the five-membered ring at higher temperatures compared to symmetrical Cp radicals such as C₅H₅^{•4} and C₅F₅^{•5}. We have previously reported the synthesis and characterization of a thermally stable *tert*-butyl-substituted Cp radical **1[•]** annulated with two homoadamantene frameworks.⁷ The X-ray analysis of this radical revealed that Jahn–Teller distortion in the five-membered ring persists even at room temperature, and the structure was characterized as a spin-localized 2,4-cyclopentadien-1-yl radical, due to the effect of σ – π conjugation between the allylic π -system (C1–C2–C3) and the carbon–carbon σ bonds in the *tert*-butyl group.

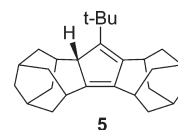


On the other hand, preliminary DFT calculations showed that the hydro and phenyl analogues (**2[•]** and **3[•]**, respectively) are C_{2v} symmetrical allyl-type radicals. This can be interpreted as arising from the absence of σ – π conjugation at C2–R in these molecules. In the present study, we prepared phenyl-substituted derivative **3[•]** from an anionic precursor **3[−]** for spectroscopic verification of the theoretical prediction. In addition, as a new reaction of a Cp radical, oxidation of **3[•]** with triplet oxygen in the presence of Ag⁺ to give a pyrylium ion is also described.

RESULTS AND DISCUSSION

Synthesis of Cp Anion **3[−].** The synthesis of the precursor cyclopentadiene **4** has been described in our previous report.⁸ When **4** was treated with KH in THF-*d*₈ under vacuum at room temperature, the solution gradually changed from colorless to pale yellow. The NMR analysis showed the quantitative formation of Cp anion **3[−]** within 1.5 h (Scheme 1). The salt K⁺**3[−]** was thermally stable under vacuum at room temperature for at least several weeks but readily reacted with H₂O to regenerate **4**.

The deprotonation of **4** was ca. 20 times faster than that of *tert*-butyl-substituted cyclopentadiene **5** under the same conditions. This can be ascribed to the greater electron-withdrawing inductive effect of the phenyl group compared to the *tert*-butyl group; the conjugative effect would be small because of its twisted conformation (see below).



Received: April 10, 2011

Published: June 23, 2011

Scheme 1

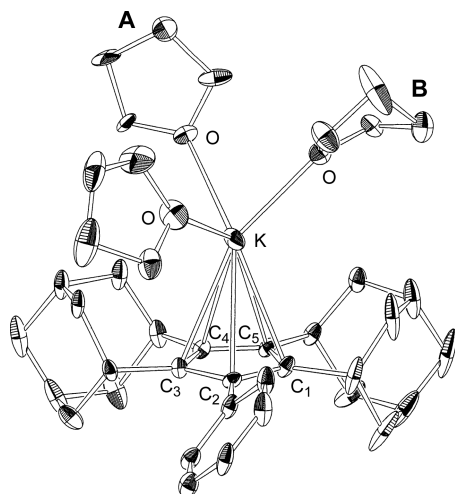
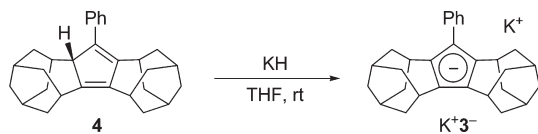


Figure 1. ORTEP drawing of $\text{K}^+\text{3}^-\bullet\text{3THF}$. Hydrogen atoms are omitted for clarity. Thermal ellipsoids are drawn at the 30% probability level. Selected bond lengths (Å) and angles (deg): C1–C2 = 1.414(8), C2–C3 = 1.419(7), C3–C4 = 1.417(7), C4–C5 = 1.408(8), C5–C1 = 1.411(8), C1–C2–C3 = 107.8(4), C2–C3–C4 = 107.7(5), C3–C4–C5 = 108.1(5), C4–C5–C1 = 108.2(5), C2–C1–C5 = 108.1(5). Two of the THF molecules, A and B, exhibited disorder, and the occupancies of disordered atoms were refined as 0.56:0.44 and 0.57:0.43, respectively.

Cooling the reaction mixture at -20°C in THF for a week in a sealed tube yielded colorless crystals of $\text{K}^+\text{3}^-\bullet\text{3THF}$, which were suitable for X-ray crystallography. X-ray analysis showed a monomeric ion pair between 3^- and K^+ , with oxygen atoms of three THF molecules coordinated to K^+ (Figure 1). Such monomeric Cp–K complexes have been previously reported only for *tert*-butyl analogue $\text{K}^+\text{1}^-\bullet\text{3THF}$ ⁷ and $(\text{PhCH}_2)_5\text{C}_5^-\text{K}^+\text{3THF}$.⁹ The formation of a polymeric chain structure, frequently observed in the crystals of Cp–K salts,¹⁰ was suppressed by the rigid and bulky substituents on the Cp ring. The twist angle between the mean plane of benzene and the Cp ring was 46° . The five-membered ring of $\text{K}^+\text{3}^-\bullet\text{3THF}$ was close to a regular pentagon, as demonstrated by the small differences among the bond lengths [$\Delta R(\text{C}–\text{C}) < 0.011 \text{ Å}$] and by the sum of the internal angles, 539.9° . Such a bond length equalization suggests significant aromaticity of Cp anion 3^- with 6π electrons, which was confirmed by a negative NICS value (-12.5), as calculated by the GIAO method at the HF/6-31G+(d,p)//B3LYP/6-31G(d) level. The distance between potassium and the Cp ring center is 2.751 Å , which is slightly larger than that in $\text{K}^+\text{1}^-\bullet\text{3THF}$ (2.739 Å)⁷ but shortened by 0.037 Å compared to $(\text{PhCH}_2)_5\text{C}_5^-\text{K}^+\text{3THF}$.⁹

Synthesis of Cp Radical 3^\bullet . The oxidation of anion 3^- with AgCl or AgSbF_6 afforded the corresponding radical 3^\bullet . A reaction carried out using 1.0 equiv of AgCl at room temperature for 10 h gave reddish orange crystals after recrystallization from hexane at -20°C (Scheme 2). Cp radical 3^\bullet was identified by ESR

Scheme 2

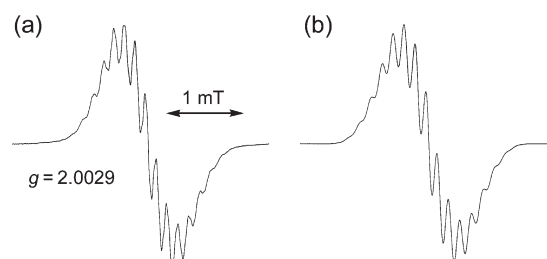
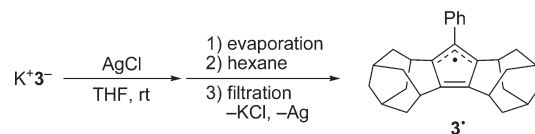


Figure 2. (a) ESR spectrum of 3^\bullet in hexane at ambient temperature. (b) Simulated ESR spectrum of 3^\bullet obtained using calculated hyperfine coupling constants shown in Figure 3 and a line with 0.056 mT .

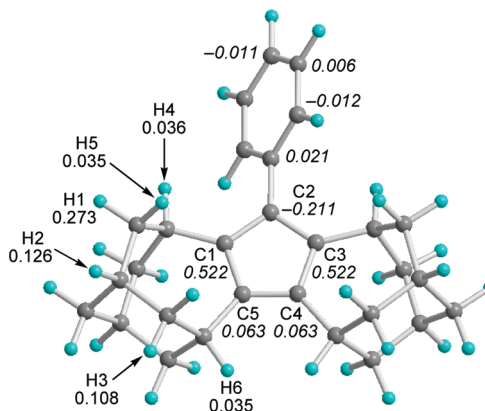
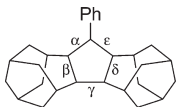


Figure 3. Structure of 3^\bullet optimized at the UB3LYP/6-31G(d) level with spin densities on carbon atoms (in italic) and ESR coupling constants (mT) of hydrogen. Coupling constants smaller than 0.03 mT were omitted.

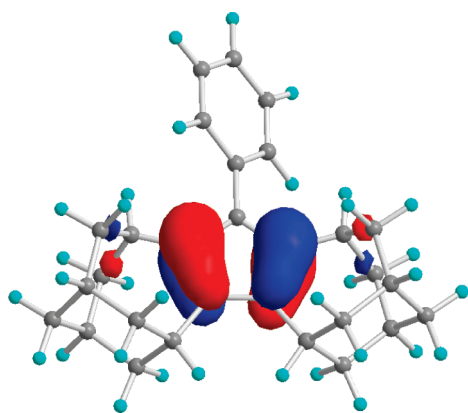
spectrum, as described below. The ^1H NMR spectrum showed only the presence of **4** with no signal of 3^\bullet observed due to significant line broadening. By comparison, the pentaisopropyl Cp radical reportedly showed broad peaks of methyl and methine protons in the ^1H NMR spectrum at δ 22.0 and 13.5, respectively.¹¹ Comparison of the amount of the Cp radical 3^\bullet in the orange solid with that of the 2,2,6,6-tetramethyl-1-piperidinyloxy radical (TEMPO) by ESR revealed that the crystalline solid contained 3^\bullet at approximately 30%. In the solid state, 3^\bullet was stable, and no decomposition took place for at least a week in air or up to 150°C under vacuum. In solution, however, it was highly air sensitive, giving a mixture of unidentified compounds.

ESR Spectrum of Cp Radical 3^\bullet . Radical 3^\bullet exhibited an ESR signal with approximately 15 lines at $g = 2.0029$ in hexane at ambient temperature (Figure 2a). A simulated spectrum (Figure 2b) based on DFT-calculated hyperfine coupling constants (Figure 3) perfectly agreed with the observed spectrum. The ESR experimental and calculation results indicated that most of the spin density is distributed equally to C1 and C3 atoms. It is

Table 1. Experimental and DFT-Calculated Bond Lengths (Å) of Cp Anion 3^- and Radical 3^\bullet


compound	method	α	β	γ	δ	ϵ
3^-	X-ray	1.419	1.417	1.408	1.411	1.414
	B3LYP ^a	1.433	1.404	1.424	1.404	1.433
3^\bullet	UB3LYP ^a	1.413	1.467	1.371	1.467	1.413

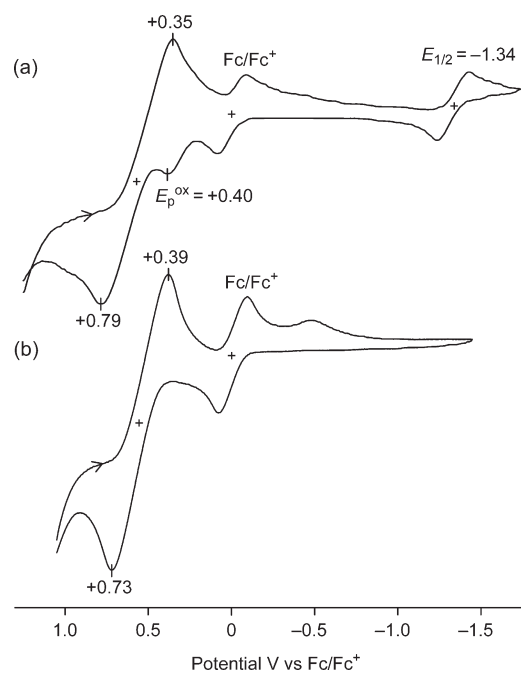
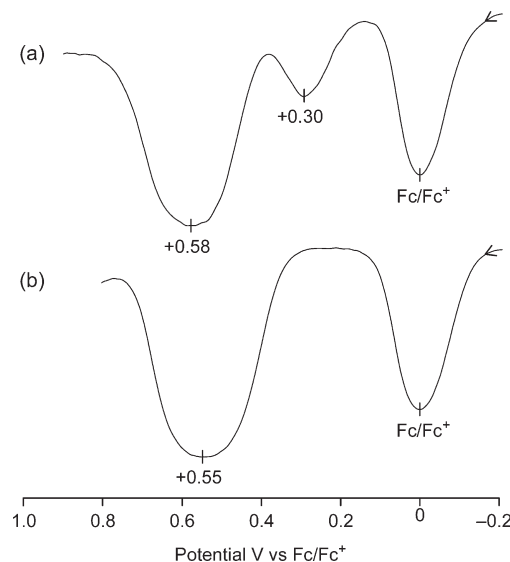
^a Calculated at the 6-31G(d) level without symmetry restrictions.

**Figure 4.** Pictorial presentation of HOMO in Cp anion 3^- .

noteworthy that the coupling constant of the *exo* proton (H1, 0.273 mT) was 8 times larger than that of the *endo* proton (H5, 0.035 mT). This can be attributed to a W-like arrangement of a C–H1 bond and the $2p_z$ orbital axis at C1, bearing a high π -spin population (Figure 3).¹² In addition, the relatively small values for the bridgehead protons H4 and H6 are due to the fact that these hydrogens lie in the plane of the Cp π system.

Bond lengths in the five-membered ring of anion 3^- and radical 3^\bullet in the DFT-optimized¹³ and X-ray structures are listed in Table 1. The predicted lengths of bonds α and ϵ in 3^\bullet are close to the values reported for symmetrical pentakis[4-(dimethylamino)pyridinium-1-yl]allyl radical [1.38(1) Å by X-ray analysis].¹⁴ There are only small differences between 3^- and 3^\bullet in the lengths of these bonds (<0.006 Å), whereas β and δ largely extend (by 0.050 and 0.056 Å, respectively) and γ shrinks by 0.037 Å upon one-electron oxidation of 3^- to 3^\bullet . These changes can be rationalized in the light of the HOMO of 3^- , which is strongly bonding at β and δ , while antibonding at γ (Figure 4). Accordingly, removal of an electron from the anion should result in an elongation of bonds β and δ and a shortening of γ , whereas the lengths of α and ϵ should not be affected.

Electrochemistry and Electronic Spectrum of Cp Radical 3^\bullet . The redox behavior of 3^\bullet was examined by cyclic voltammetry (Figure 5) and differential pulse voltammetry (Figure 6) in vacuum-degassed CH_2Cl_2 at -78°C . Comparison of cyclic voltammograms between 3:7 mixture of 3^\bullet and 4 and pure cyclopentadiene 4¹⁵ indicated that radical 3^\bullet showed an irreversible oxidation wave and a reversible reduction wave at $E_p^{\text{ox}} = +0.40$ and $E_{1/2} = -1.34$ V ($E_p^{\text{red}} = -1.43$ V) vs Fc/Fc⁺, respectively. Although high scan rates and low temperatures

**Figure 5.** Cyclic voltammograms of (a) a 3:7 mixture of 3^\bullet and 4 ($[3^\bullet] = 8 \times 10^{-4}$ M, -78°C , scan rate 200 mV/s) and (b) pure 4 (2×10^{-3} M, room temperature, scan rate 100 mV/s). Both voltammograms were taken in degassed ($<10^{-4}$ mmHg) CH_2Cl_2 using TBAP (0.1 M) and ferrocene (1×10^{-3} M) as a supporting electrolyte and an internal potential reference, respectively. Three Pt wires (0.6 mm diameter) were used for the working, counter, and auxiliary reference electrodes.**Figure 6.** Differential pulse voltammograms of (a) a 3:7 mixture of 3^\bullet and 4 at -78°C and (b) pure 4 at room temperature taken under conditions identical to those used in Figure 5. Scan rate 20 mV/s.

were used in the hope that a reversible oxidation might be observed, the wave remained irreversible even at -78°C with scan rates up to 500 mV/s. These findings indicate that the reduction product, that is, Cp anion 3^- is stable while the corresponding cation formed by one-electron oxidation is unstable due to antiaromaticity. The oxidation and reduction peak

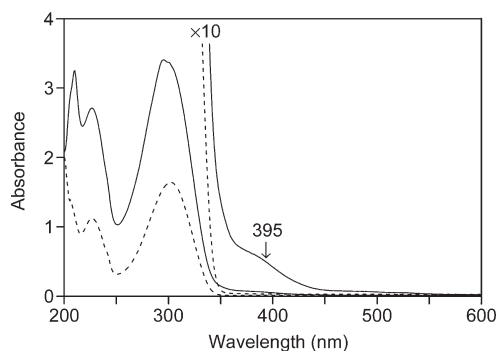
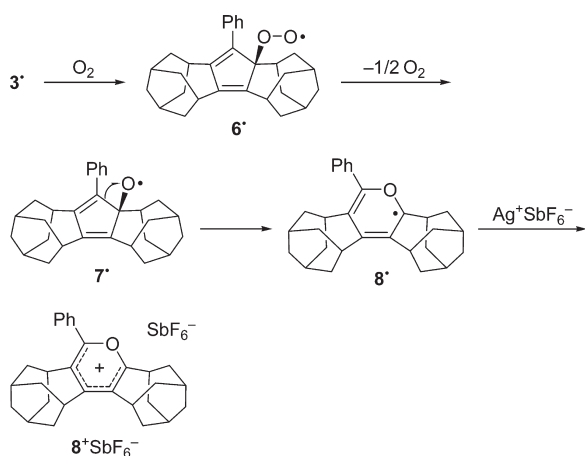


Figure 7. Electronic absorption spectra of a 27:73 mixture of **3*** and **4** (solid line, $[3^*] = 9.0 \times 10^{-5} \text{ M}$) and pure **4** (dashed line, $1.48 \times 10^{-4} \text{ M}$) in hexane. Cell length, 1 cm.

Scheme 3



potentials of **3*** are more positive by 0.03 and 0.35 V, respectively, than that of the *tert*-butyl analogue **1*** ($E_p^{\text{ox}} = 0.37 \text{ V}$; $E_p^{\text{red}} = -1.78 \text{ V}$)⁷ because of the inductive and conjugative effects of the phenyl group. This tendency is also predictable from the lowering of the HOMO and LUMO levels of **3*** (by 0.05 and 0.15 eV, respectively) compared to **1***.

Comparison of the UV–vis absorption spectra (Figure 7) between a mixture of radical **3*** and cyclopentadiene **4** (solid line) and pure **4** (dashed line) in hexane under vacuum showed that radical **3*** has a shoulder absorption at 395 nm (ϵ 520). This absorption was assigned to HOMO(β)→LUMO+1(β) transition (405 nm, 3.06 eV) with an oscillator strength of $f = 0.0079$ based on the theoretical calculations [UCIS/6-31G(d)//UB3LYP/6-31G(d)].

Reaction of Cp Radical **3* with Molecular Oxygen in the Presence of $\text{Ag}^+\text{SbF}_6^-$.** When radical **3*** was exposed to air in the presence of $\text{Ag}^+\text{SbF}_6^-$ at room temperature, pyrylium ion salt 8^+SbF_6^- was obtained as stable colorless crystals in a 39% yield based on consumed precursor **4** (Scheme 3). The structure of 8^+SbF_6^- was confirmed by its NMR spectrum, elemental analysis, and X-ray crystallography (Figure 8). Natural population analysis with DFT method demonstrated that most of the positive charge is on C1, C3, and C5 (0.39, 0.12, and 0.49, respectively). In accord with this result, GIAO calculations predicted low-field shift of the ^{13}C NMR signals of these carbons (δ 175.9, 189.8, and 193.6, respectively), which is in agreement with

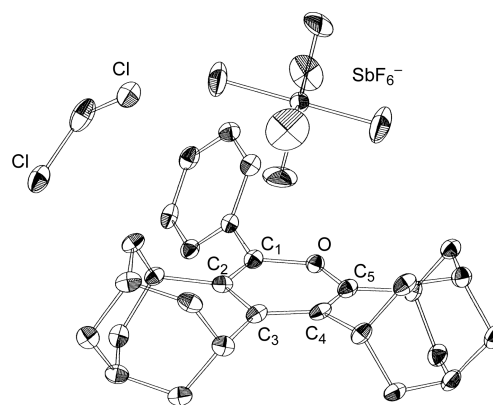


Figure 8. ORTEP drawing of $8^+\text{SbF}_6^- \cdot \text{CH}_2\text{Cl}_2$. Hydrogen atoms are omitted for clarity. Thermal ellipsoids are drawn at the 30% probability level for non-hydrogen atoms. Selected bond lengths (Å) and angles (deg): C1–C2 = 1.370(10), C2–C3 = 1.456(10), C3–C4 = 1.409(11), C4–C5 = 1.382(11), C1–O = 1.368(8), O–C5 = 1.347(8), C1–C2–C3 = 117.5(7), C2–C3–C4 = 119.1(7), C3–C4–C5 = 118.7(7), O–C5–C4 = 120.9(7), C1–O–C5 = 121.7(6), O–C1–C2 = 121.3(6). The anion SbF_6^- exhibited disorder, and the occupancies of disordered atoms were refined as 0.68:0.32.

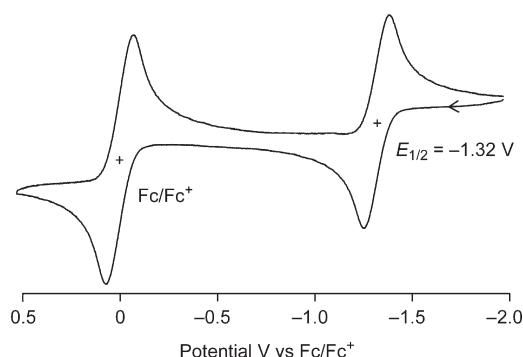


Figure 9. Cyclic voltammogram of 8^+SbF_6^- ($2 \times 10^{-4} \text{ M}$) measured in CH_2Cl_2 at room temperature under Ar with a glassy carbon working electrode (3 mm diameter). Supporting electrolyte, TBAP (0.1 M). Scan rate, 100 mV/s.

experimental observation of three deshielded signals at δ 184.3, 179.0, and 166.8. The proposed mechanism of the oxidation begins with the addition of dioxygen to the Cp ring to form a peroxy radical **6***, the intermolecular reaction of which brings about the loss of an oxygen atom¹⁶ to lead to cyclopentadienyloxy radical **7***. The subsequent rearrangement forms the pyrylium radical **8***,¹⁷ followed by oxidation by Ag^+ to afford a stable 6π aromatic cation **8***. There are only a few examples of the product study for the reaction of Cp radical with an oxygen molecule. It is known that exposure of the $(i\text{-Pr})_5\text{C}_5^*$ radical to oxygen yields a peroxy radical $(i\text{-Pr})_5\text{C}_5\text{OO}^*$, which releases an isopropoxy radical to afford tetraisopropylcyclopentadienone as the stable final product.¹¹

Cyclic voltammetry of 8^+SbF_6^- showed a reversible reduction at $E_{1/2} = -1.32 \text{ V}$ vs Fc/Fc^+ (Figure 9). For comparison, 2,6-di-*tert*-butyl-4-methylpyrylium ion is reportedly reduced only irreversibly at $E_{\text{pc}} = -1.16 \text{ V}$ vs Fc/Fc^+ ,¹⁸ which is ascribed to ready dimerization of the corresponding radical at C4.²¹ In the case of **8***, the steric hindrance by the homoadamantene frameworks prevents the corresponding radical **8*** from dimerization.

More negative reduction potential of 8^+ also shows higher stability of this cation due to σ - π conjugation, which is consistent with the mechanistic proposal in Scheme 3 that radical 8^\bullet is readily oxidized by Ag^+ to 8^+ .

CONCLUSION

Phenyl-substituted Cp radical 3^\bullet , annelated with two homoadamantene units, was prepared. ESR analysis indicated that the two homoadamantene frameworks in 3^\bullet are equivalent and the C1–C2(Ph)–C3 moiety of the five-membered ring is a symmetrical, allyl-like radical. This is in contrast to the *tert*-butyl analogue 1^\bullet possessing a spin-localized nature in which σ - π conjugation is present. The reaction of Cp radical 3^\bullet with an oxygen molecule in the presence of $Ag^+SbF_6^-$ afforded a new pyrylium salt $8^+SbF_6^-$, which is a new reaction mode for a Cp radical with oxygen. To the best of our knowledge, the transformation of Scheme 3 represents a new pathway for the air oxidation of a Cp radical.

EXPERIMENTAL SECTION

Preparation and Characterization of Cyclopentadienide Ion 3^- . An NMR sample tube containing cyclopentadiene 4^8 (38.1 mg, 0.10 mmol) and KH (6.1 mg, 0.15 mmol) was evacuated with a vacuum line. Tetrahydrofuran- d_8 (0.75 mL), dried with a potassium mirror and degassed by repeated freeze–pump–thaw cycles, was vacuum-transferred to the NMR sample tube. The tube was sealed under vacuum, and the reaction was monitored at room temperature by 1H NMR, which showed the quantitative formation of 3^- within 1.5 h. Colorless crystals suitable for X-ray analysis were obtained by cooling this solution to $-20^\circ C$: 1H NMR (300 MHz, THF- d_8) δ 7.06 (t, $J = 7.4$ Hz, 2H), 6.90 (d, $J = 7.8$ Hz, 2H), 6.71 (t, $J = 7.1$ Hz, 1H), 3.02 (br s, 2H), 2.87 (br s, 2H), 2.14–1.60 (m, 24H); ^{13}C NMR (75.5 MHz, THF- d_8) δ 144.6, 130.4, 127.8, 123.4, 120.5, 120.2, 114.0, 39.9, 39.6, 39.5, 31.8, 31.7, 31.4.

Preparation and Characterization of Cyclopentadienyl Radical 3^\bullet . This experiment was carried out using a two-chamber reaction vessel connected to a vacuum line. Cyclopentadiene 4 (191 mg, 0.50 mmol) and KH (20.0 mg, 0.50 mmol) were placed in one chamber, $AgCl$ (70.2 mg, 0.49 mmol) in the other, and the apparatus was evacuated ($<10^{-4}$ mmHg). Tetrahydrofuran (4.0 mL), dried with a potassium mirror and degassed by repeated freeze–pump–thaw cycles, was distilled into the former chamber to allow 4 to react with KH. After 14 h, the solution of anion 3^- thus prepared was transferred to the latter chamber to allow oxidation, and the mixture was stirred in the dark for 10 h. From the solution of 3^\bullet thus obtained, the THF was evaporated under reduced pressure, and the apparatus was opened to an argon atmosphere in a glovebox. The product was dissolved in hexane and filtered through a PTFE membrane filter to remove Ag and KCl . The filtrate was cooled to $-20^\circ C$ to give 7.9 mg of reddish orange crystals, which were shown to consist of 3^\bullet and 4 (27:73) from the ESR signal intensity using TEMPO as a standard.

Preparation and Isolation of Pyrylium Salt $8^+SbF_6^-$. A THF solution of 3^\bullet was prepared from 46.3 mg (0.12 mmol) of 4 , 5.1 mg (0.13 mmol) of KH, and 42.1 mg (0.12 mmol) of $Ag^+SbF_6^-$ by the method described above. The apparatus was opened to air, and the THF was removed under reduced pressure. The residue was purified by chromatography on silica gel (hexane and CH_2Cl_2) to afford 22.9 mg of 4 and 15.2 mg of $8^+SbF_6^-$ (39% based on consumed 4). Recrystallization of from hexane– CH_2Cl_2 gave colorless crystals suitable for X-ray analysis: mp $305^\circ C$ dec, 1H NMR (300 MHz, $CDCl_3$) δ 7.70–7.52 (m, 5H), 3.71 (t, $J = 6.2$ Hz, 1H), 3.57 (t, $J = 6.5$ Hz, 1H), 3.47–3.34 (m, 2H), 2.34–1.78 (m, 24H); ^{13}C NMR (75.5 MHz, $CDCl_3$) δ 184.3, 179.0, 166.8, 141.3, 140.9, 132.1, 130.2, 129.4, 129.1, 41.2, 35.6, 34.6, 34.5, 33.9,

33.5, 32.6, 32.4, 31.6, 30.5, 27.3, 27.2; IR (KBr, cm^{-1}) 2910, 2855, 1607, 1590, 1576, 1510, 1502, 1472, 1447, 952, 698, 659. Anal. Calcd for $C_{29}H_{33}F_6OSb$: C, 55.00; H, 5.25. Found: C, 54.67; H, 5.12.

X-ray Crystal Structure Analysis. Intensity data were collected at 100 K on a Bruker SMART APEX diffractometer with Mo K α radiation and a graphite monochromator. The structures were solved by direct method (SHELXTL) and refined by the full-matrix least-squares on F^2 (SHELXL-97). All non-hydrogen atoms were refined anisotropically, and hydrogen atoms were placed using AFIX instructions and refined isotropically.

$K^+3^- \cdot 3THF$: $C_{41}H_{57}KO_3$; FW = 636.97, crystal size $0.20 \times 0.20 \times 0.20$ mm³, monoclinic, Cc , $a = 10.771(5)$ Å, $b = 18.247(5)$ Å, $c = 17.767(5)$ Å, $\alpha = 90.000^\circ$, $\beta = 93.433(5)^\circ$, $\gamma = 90.000^\circ$, $V = 3486(2)$ Å³, $Z = 4$, $D_c = 1.214$ g/cm³. The refinement converged to $R_1 = 0.0803$, $wR_2 = 0.2368$ ($I > 2\sigma(I)$), GOF = 1.453. Two of the THF molecules exhibited disorder, and the occupancies of disordered atoms were refined as 0.56:0.44 and 0.57:0.43, respectively.

$8^+SbF_6^- \cdot CH_2Cl_2$: $C_{30}H_{35}Cl_2F_6OSb$; FW = 718.23, crystal size $0.30 \times 0.30 \times 0.20$ mm³, monoclinic, $P2(1)/c$, $a = 13.787(3)$ Å, $b = 15.652(4)$ Å, $c = 15.063(4)$ Å, $\alpha = 90^\circ$, $\beta = 112.361(4)^\circ$, $\gamma = 90^\circ$, $V = 3006(12)$ Å³, $Z = 4$, $D_c = 1.587$ g/cm³. The refinement converged to $R_1 = 0.0664$, $wR_2 = 0.1492$ ($I > 2\sigma(I)$), GOF = 1.125. The SbF_6^- moiety exhibited disorder, and the occupancies of disordered atoms were refined as 0.68:0.32.

Calculations. Density functional theory (DFT) calculations²² were performed using the Gaussian 98 program.²³ Structures were optimized at the B3LYP/6-31G(d) and UB3LYP/6-31G(d) levels for molecules with spin multiplicities 1 and 2, respectively. The resulting geometries were verified by frequency calculations to have no imaginary frequencies. The energies, atomic charges (NBO), and NMR chemical shifts (GIAO) were computed by single-point calculations for these geometries using the (U)B3LYP/6-311+G(d,p) level. For the calculations of NICS values of 3^- and absorption wavelengths of 3^\bullet , the HF/6-31G+(d,p) and UCIS/6-31G(d) levels were used, respectively.

ASSOCIATED CONTENT

S Supporting Information. 1H and ^{13}C NMR spectra and crystallographic data (tables and CIF files) for K^+3^- and $8^+SbF_6^-$ and the results of DFT calculations for 2^\bullet , 3^- , 3^\bullet , 7^\bullet , 8^\bullet , and 8^+ . This material is available free of charge via the Internet at <http://pubs.acs.org>.

AUTHOR INFORMATION

Corresponding Author

*E-mail: kitagawa@chem.mie-u.ac.jp.

ACKNOWLEDGMENT

This work was supported by a Grant-in-Aid for Scientific Research from the Ministry of Education, Culture, Sports, Science and Technology, Japan.

REFERENCES

- (1) For example, see: (a) Schott, A.; Schott, H.; Wilke, G.; Brandt, J.; Hoberg, H.; Hoffmann, E. G. *Justus Liebig's Ann. Chem.* **1973**, 508. (b) Lowack, R. H.; Vollhardt, K. P. C. *J. Organomet. Chem.* **1994**, 476, 25. (c) Sitzmann, H.; Dezember, T.; Ruck, M. *Angew. Chem., Int. Ed.* **1998**, 37, 3114. (d) Lamansky, S.; Thompson, M. E. *Chem. Mater.* **2002**, 14, 109.
- (2) (a) Borden, W. T.; Davidson, E. R. *J. Am. Chem. Soc.* **1979**, 101, 3771. (b) Bearpark, M. J.; Robb, M. A.; Yamamoto, N. *Spectrochim. Acta A* **1999**, 55, 639. (c) Applegate, B. E.; Miller, T. A.; Barckholtz, T. A.

J. Chem. Phys. **2001**, *114*, 4855. (d) Applegate, B. E.; Bezant, A. J.; Miller, T. A. *J. Chem. Phys.* **2001**, *114*, 4869. (e) Zilberg, S.; Haas, Y. *J. Am. Chem. Soc.* **2002**, *124*, 10683.

(3) Snyder, L. C. *J. Chem. Phys.* **1960**, *33*, 619.

(4) (a) Liebling, G. R.; McConnell, H. M. *J. Chem. Phys.* **1965**, *42*, 3931. (b) Hedaya, E. *Acc. Chem. Res.* **1969**, *2*, 367.

(5) Chen, T.; Günthard, Hs. H. *Chem. Phys.* **1985**, *97*, 187.

(6) (a) Kira, M.; Watanabe, M.; Sakurai, H. *J. Am. Chem. Soc.* **1977**, *99*, 7780. (b) Kira, M.; Watanabe, M.; Sakurai, H. *J. Am. Chem. Soc.* **1980**, *102*, 5202. (c) Barker, P. J.; Davies, A. G.; Tse, M.-W. *J. Chem. Soc., Perkin Trans. 2* **1980**, 941.

(7) Kitagawa, T.; Ogawa, K.; Komatsu, K. *J. Am. Chem. Soc.* **2004**, *126*, 9930.

(8) Ogawa, K.; Minegishi, S.; Komatsu, K.; Kitagawa, T. *J. Org. Chem.* **2008**, *73*, 5248.

(9) Lorberth, J.; Shin, S.-H.; Wocadlo, S.; Massa, W. *Angew. Chem., Int. Ed. Engl.* **1989**, *28*, 735.

(10) (a) Jutzi, P.; Burford, N. *Chem. Rev.* **1999**, *99*, 969. (b) Harder, S. *Coord. Chem. Rev.* **1998**, *176*, 17. **2000**, *199*, 331 (erratum).

(11) (a) Sitzmann, H.; Boese, R. *Angew. Chem., Int. Ed. Engl.* **1991**, *30*, 971. (b) Sitzmann, H.; Bock, H.; Boese, R.; Dezember, T.; Havlas, Z.; Kaim, W.; Moscherosch, M.; Zanathy, L. *J. Am. Chem. Soc.* **1993**, *115*, 12003.

(12) (a) Gerson, F.; Lopez, J.; Akaba, R.; Nelsen, S. F. *J. Am. Chem. Soc.* **1981**, *103*, 6716. (b) Nishinaga, T.; Wakamiya, A.; Yamazaki, D.; Komatsu, K. *J. Am. Chem. Soc.* **2004**, *126*, 3163.

(13) Based on the fact that the structure of *tert*-butyl analogue **1**[•] was reproduced very well by DFT calculations at the UB3LYP/6-31G(d) level (ref 7), the structure of **3**[•] having a C₂ symmetry is considered reliable.

(14) DiMugno, S. G.; Waterman, K. C.; Speer, D. V.; Streitwieser, A. *J. Am. Chem. Soc.* **1991**, *113*, 4679.

(15) The significantly large intensity and peak-to-peak separation for **4** ($E_{\text{p}}^{\text{ox}} - E_{\text{p}}^{\text{red}} = 0.34$ V) may be due to a fast chemical process after oxidation.

(16) (a) Ingold, K. U. In *Free Radicals*; Kochi, J. K., Ed.; John Wiley and Sons: New York, 1973; Vol. 1, p 59. (b) Kitagawa, T.; Miyabo, A.; Fujii, H.; Okazaki, T.; Mori, T.; Matsudou, M.; Sugie, T.; Takeuchi, K. *J. Org. Chem.* **1997**, *62*, 888.

(17) DFT calculation at the UB3LYP/6-311+G(d,p)//UB3LYP/6-31(d) level estimated that pyrylium radical **8**[•] is more stable by 23.3 kcal/mol than cyclopentadienyloxy radical **7**[•], which supports this rearrangement.

(18) Evaluated from the originally reported value, −0.76 V vs SCE (ref 19), and the potential of Fc/Fc⁺ couple, 0.40V vs SCE (ref 20).

(19) Detty, M. R.; McKelvey, J. M.; Luss, H. R. *Organometallics* **1988**, *7*, 1131.

(20) Connelly, N. G.; Geiger, W. E. *Chem. Rev.* **1996**, *96*, 877.

(21) Pragst, F.; Ziebig, R.; Seydewitz, U.; Driesel, G. *Electrochim. Acta* **1980**, *25*, 341.

(22) Koch, W.; Holthausen, M. C. *A Chemist's Guide to Density Functional Theory*, 2nd ed.; Wiley-VCH: Weinheim, Germany, 2000.

(23) Frisch, M. J.; Trucks, G. W.; Schlegel, H. B.; Scuseria, G. E.; Robb, M. A.; Cheeseman, J. R.; Zakrzewski, V. G.; Montgomery, J. A., Jr.; Stratmann, R. E.; Burant, J. C.; Dapprich, S.; Millam, J. M.; Daniels, A. D.; Kudin, K. N.; Strain, M. C.; Farkas, O.; Tomasi, J.; Barone, V.; Cossi, M.; Cammi, R.; Mennucci, B.; Pomelli, C.; Adamo, C.; Clifford, S.; Ochterski, J.; Petersson, G. A.; Ayala, P. Y.; Cui, Q.; Morokuma, K.; Salvador, P.; Dannenberg, J. J.; Malick, D. K.; Rabuck, A. D.; Raghavachari, K.; Foresman, J. B.; Cioslowski, J.; Ortiz, J. V.; Baboul, A. G.; Stefanov, B. B.; Liu, G.; Liashenko, A.; Piskorz, P.; Komaromi, I.; Gomperts, R.; Martin, R. L.; Fox, D. J.; Keith, T.; Al-Laham, M. A.; Peng, C. Y.; Nanayakkara, A.; Challacombe, M.; Gill, P. M. W.; Johnson, B.; Chen, W.; Wong, M. W.; Andres, J. L.; Gonzalez, C.; Head-Gordon, M.; Replogle, E. S.; Pople, J. A. *Gaussian 98*, revision A.11; Gaussian, Inc.: Pittsburgh PA, 2001.